PTEP

Prog. Theor. Exp. Phys. **2019**, 053E01 (9 pages)
DOI: 10.1093/ptep/ptz032

Ion Bernstein mode instability with ring velocity distribution function

N. Noreen*, F. Riaz, S. Malik, and S. Zaheer

Forman Christian College (A Chartered University), Ferozpur Road, Lahore, 54600 Pakistan
*E-mail: nailanoreen@fccollege.edu.pk

Received October 30, 2018; Revised March 8, 2019; Accepted March 10, 2019; Published May 11, 2019

The Bernstein mode instability plays a vital role in tokamaks and space plasma regimes like Jovian planets and interstellar space. We introduce the contributions of ions along with electrons with the help of a ring velocity distribution function. We conclude that the ions play a significant role in shifting the threshold frequency value toward the lower-wavelength regime. In comparison with the electron Bernstein mode, it is concluded that the electron mode becomes unstable for higher wavelengths, but on the contrary the ion Bernstein mode tries to be more stable at low frequencies. The growth rate has been calculated analytically as well as numerically. A graphical comparison provides us with a detailed view of the unstable regions. The growth rates demonstrate that the mode becomes more unstable, while increasing the value of the frequency ratio $(\omega_{pi}/\Omega_e)^2$.

Subject Index E10, E13

1. Introduction

The subject of heating effects of magnetized plasmas is a deep-rooted topic, dating from the early 1950s with the start of the controlled fusion program. The Bernstein mode can be completely absorbed on the wings of the cyclotron resonance [1,2]. The ion Bernstein wave, i.e., a hot plasma wave, is used to carry radio-frequency power to heat a tokamak reactor core. Current-driven electron Bernstein wave heating in spherical tokamaks has been explored because the high density and low magnetic field configuration of these machines make the plasma inaccessible to the ordinary and extraordinary modes used in standard tokamaks [3].

The problem of perpendicularly propagated electron oscillations with an external magnetic field has been discussed by Gross [4] and Sen [5]. Gross claimed to find Landau damping whose wavelength is less than the standard Debye length. Later, Bernstein [6] found some errors in Gross's [4] conclusion. He calculated the Bernstein mode with a Maxwellian distribution function and observed its stability analysis. That work also treated fully ionized small amplitude oscillations in collisionless plasma in the presence of an external magnetic field.

Crawford et al. [7] formulated the dispersion relation of the Bernstein mode with a delta function, i.e., a transverse electron velocity distribution. This formulation shows that an unstable wave may lead to the growing wave phenomena in finite plasmas due interaction with slow wave circuits. Even in an infinite plasma, modes couple with each other, leading to wave growth. Later, Crawford [8] predicted theoretically that cyclotron harmonic waves should propagate in warm plasma confined by a magnetic field, showing cutoff and resonance behavior associated with harmonics of the cyclotron frequency and the upper hybrid resonance frequency.

Ram et al. [9] proved that the Bernstein mode can be excited by mode conversion of either an extra-ordinary mode or an ordinary mode. Keston et al. [10] used weakly relativistic plasmas to produce the dispersion relation for the electrostatic Bernstein mode with full momentum dependence of the cyclotron frequency. Later, Laing et al. [11] showed that these modes are not completely undamped but have a small negative definite imaginary component close to the rest cyclotron harmonic.

Cairns et al. [1] explained that the Bernstein waves possess high perpendicular wave numbers which reduce trapping. Efthimion [12] explained that electron Bernstein waves have the potential to heat and drive current for high-β plasmas. Deeba et al. [13] also calculated the electron Bernstein mode with an (r, q) distribution function. Ali et al. [14] investigated the Bernstein mode in relativistic degenerate plasmas. They discussed the cases in non-relativistic and ultra-relativistic regimes and proved that Bernstein waves and upper hybrid oscillations can be modified by increasing the number density.

Crawford [7] and Leuterer [15] reported for the first time the presence of electron Bernstein waves in a laboratory plasma in 1965 and 1969 respectively. Such waves have also been observed by spacecraft, having been emitted from the magnetized plasma of Io, a moon of Jupiter [16]. Mace [17] studied the electron Bernstein wave for an isotropic kappa distribution function.

Bernstein waves, which are electrostatic in nature and are observed in the electron cyclotron harmonic frequency range, propagate perpendicularly to the ambient magnetic field. These waves have been observed in Li neutral gas release in the solar wind. Meyer-Vernet et al. [18] discussed that the weakly banded emission from the Jupiter magnetosphere and between consecutive gyroharmonic frequencies is quasithermal noise in a Bernstein wave. Recent observations have been made by the Voyager spacecraft of electrostatic waves in Jupiter's magnetosphere [19]. Electrostatic electron and ion cyclotron harmonic waves have been observed by Voyager II in the magnetosphere of Neptune. The electron Bernstein wave generated by a loss cone distribution is scrambled to Neptune's parameters, and a comparison of the theory with the observed electron flux indicates good agreement [20]. These results were based on Voyager data from the outer planets. Bernhard et al. [21] observed the transmission of high-power electromagnetic waves from the HAARP facility in Alaska.

It was assumed that Maxwellian plasma always supports the Bernstein wave, so that the real frequency can be given by classical Bernstein wave solutions. But the growth rate can determined by a very small number of electrons, so many types of perpendicular distribution function can be used [22]. For f_0 we will use the ring distribution function [23–25]; in a weakly collisional plasma the ring distribution may be a source of free energy for instabilities, due to effective temperature anisotropies and streaming [26]:

$$f_0 = \frac{1}{2\pi \hat{v}_\perp} \delta(v_\perp - \hat{v}_\perp)\delta(\hat{v}_\parallel - v_\parallel). \tag{1}$$

In the literature the distribution function has been used for relativistic calculations of Bernstein waves [22–24,27]. But evidence of a non-relativistic formulation is also available [22,25]. The parallel part of the distribution function participates in a relativistic version of the Bernstein mode in a cold plasma regime but has no contribution to the non-relativistic calculation [22].

The layout of this paper is as follows: In Sect. 2 we use the kinetic theory to calculate the general dispersion relation for magnetized plasma. We derive analytical expressions for the dielectric constant by using ring distribution functions. A brief summary of the results and a discussion are given in Sect. 3.

2. Mathematical formulation

We follow the general formalism of kinetic theory to evaluate the instability of the Bernstein wave in a hot magnetized plasma. For the Bernstein wave the relevant component of the generalized dielectric tensor is [27–31]

$$\epsilon_{xx} = 1 - \sum_{\alpha} \frac{2\pi}{s} m\omega_{p\alpha}^2 \int_{-\infty}^{\infty} dv_{\parallel} \int_{0}^{\infty} v_{\perp} dv_{\perp} \chi_1 \sum_{n=-\infty}^{\infty} \frac{M_{xx}}{(s + ik_{\parallel}v_{\parallel} + in\omega_{c\alpha})}, \tag{2}$$

where $M_{xx} = \frac{n^2}{z_{\alpha}^2} v_{\perp} [J_n(z_{\alpha})]^2$, $z_{\alpha} = \frac{k_{\perp}v_{\perp}}{\omega_{c\alpha}}$, $\chi_1 = \frac{\partial f_0}{\partial v_{\perp}} + \frac{ik_{\parallel}}{s}\left(v_{\parallel}\frac{\partial f_0}{\partial v_{\perp}} - v_{\perp}\frac{\partial f_0}{\partial v_{\parallel}}\right)$, and $s = -i\omega$.

Since we are dealing with perpendicular propagation, $k_{\parallel} = 0$ so $\chi_1 = \frac{\partial f_0}{\partial v_{\perp}}$, where $\omega_{p\alpha}$ and $\omega_{c\alpha}$ are the plasma and gyro frequencies respectively, and α shows the species, i.e., electron or ion.

Simplifying, we get

$$1 + \sum_{\alpha} \frac{4\pi\omega_{p\alpha}^2 m^2}{k_{\perp}^2} \sum_{n=1}^{\infty} \frac{n^2\omega_{c\alpha}^2}{(\omega^2 - n^2\omega_{c\alpha}^2)} \int_{-\infty}^{\infty} dv_{\parallel} \int_{0}^{\infty} dv_{\perp} J_n^2(z_{\alpha}) \frac{\partial f_0}{\partial v_{\perp}} = 0, \tag{3}$$

where f_0 is the distribution function, and in this case the ring distribution function has been used:

$$f_0 = \frac{1}{2\pi\hat{v}_{\perp}} \delta(v_{\perp} - \hat{v}_{\perp})\delta(\hat{v}_{\parallel} - v_{\parallel}).$$

As the parallel streaming has no effect on the non-relativistic ion Bernstein mode, we obtain the dispersion relation for the Bernstein wave after performing simple integrations:

$$1 - \sum_{\alpha} \frac{\omega_{p\alpha}^2}{\omega^2} \sum_{n=1}^{\infty} \frac{2n^2 J_n(\hat{z}_{\alpha}) J_n'(\hat{z}_{\alpha})}{\hat{z}_{\alpha}} \left[\frac{2\omega^2}{(\omega^2 - n^2\omega_{c\alpha}^2)}\right] = 0. \tag{4}$$

At a lower frequency range, the harmonics of the ion cyclotron frequency exhibit similar properties to the electron Bernstein wave. The ion contribution in the dispersion relation can be neglected in the high-frequency range, but the electron contribution persists even at low frequencies. So, there is not a complete symmetry between the two types of Bernstein waves [30]. Opening out the sum over species $\sum_{\alpha}$ for electrons and ions:

$$\begin{aligned} 1 = {} & \frac{\omega_{pe}^2}{\omega^2} \sum_{n\,=\,1}^{\infty} \frac{2n^2 J_n\left(\hat{z}_e\right) J_n'\left(\hat{z}_e\right)}{\hat{z}_e} \left(\frac{2\omega^2}{\omega^2 - n^2\omega_c^2}\right) \\ & + \frac{\omega_{pi}^2}{\omega^2} \sum_{n\,=\,1}^{\infty} \frac{2n^2 J_n\left(\hat{z}_i\right) J_n'\left(\hat{z}_i\right)}{\hat{z}_i} \left(\frac{2\omega^2}{\omega^2 - n^2\Omega_c^2}\right), \end{aligned} \tag{5}$$

where ω_c represents the electron gyro frequency and Ω_c the ion gyro frequency, and ω_{pe}^2 and ω_{pi}^2 are the plasma frequencies for electrons and ions respectively. The value of $J_n'\left(\hat{z}_{i,e}\right)$ as $\hat{z}_{i,e} \to 0$ is given by $J_n'\left(\hat{z}_{i,e}\right) = \frac{n}{\hat{z}_{i,e}} J_n\left(\hat{z}_{i,e}\right)$; for electrons, $\hat{z}_e = \frac{k_{\perp}\hat{v}_{\perp}}{\omega_c}$, and for ions, $\hat{z}_i = \frac{k_{\perp}\hat{v}_{\perp}}{\Omega_c}$. By applying the small-$\hat{z}$ argument expansion as $\hat{z} \to 0$, and (per Chen [30]) considering only the $n = 1$ term,

$$1 = \frac{\omega_{pe}^2}{\omega^2 - \omega_c^2} + \frac{\omega_{pi}^2}{\omega^2} \sum_{n\,=\,1}^{\infty} \frac{2n^2 J_n\left(\hat{z}_i\right) J_n'\left(\hat{z}_i\right)}{\hat{z}_i} \left(\frac{2\omega^2}{\omega^2 - n^2\Omega_c^2}\right). \tag{6}$$

By applying these approximations, the first part of Eq. (6) reduces to the upper hybrid mode, as explained by Bashir et al. [22]. By following Chen [30] and separating out the $n = 1$ term for the ion Bernstein mode, we obtain

$$1 = \frac{\omega_{pe}^2}{\omega^2 - \omega_c^2} + \frac{\omega_{pi}^2}{\omega^2 - \Omega_c^2} + \frac{\omega_{pi}^2}{\omega^2} \sum_{n=2}^{\infty} \frac{2n^2 J_n\left(\hat{z}_i\right) J_n'\left(\hat{z}_i\right)}{\hat{z}_i} \left(\frac{2\omega^2}{\omega^2 - n^2\Omega_c^2}\right). \tag{7}$$

This result is in good agreement with the Maxwellian results of Chen [30].

3. Results and discussion

By numerically solving Eq. (7), we can separate the real and imaginary parts of the wave as $\omega = \omega_r + i\omega_i$. The imaginary part plays a significant role in estimating the threshold value and determining the purely growing mode, i.e., $\omega_r = 0$ [32–34].

Figure 1 shows the stability of the ion Bernstein mode for ω_r/Ω_c vs. $\hat{z}_i = k_\perp \hat{v}_\perp/\Omega_c$, showing that at $\omega_{pi}^2/\Omega_c^2 = 11.0$ the wave is stable, but Fig. 2 shows that the variation of the frequency range in the real part of wave creates intersections of branches. The first intersection point can easily be observed at $\omega_{p_i}^2/\Omega_c^2 = 11.5$; this is the threshold value for instability of the ion Bernstein wave. During overlapping of wave branches in real frequencies the wave becomes unstable and gaps are generated between the harmonics, as discussed by Bashir et al. [22]. According to Bashir et al. [22] and Crawford [35], the threshold point for the electron Bernstein wave is $\omega_{p_e}^2/\omega_c^2 = 6.63$, while for the ion Bernstein wave the threshold value is $\omega_{p_i}^2/\Omega_c^2 = 11.5$, where $\omega_{p_i}^2/\Omega_c^2$ and $\omega_{p_e}^2/\omega_c^2$ are the

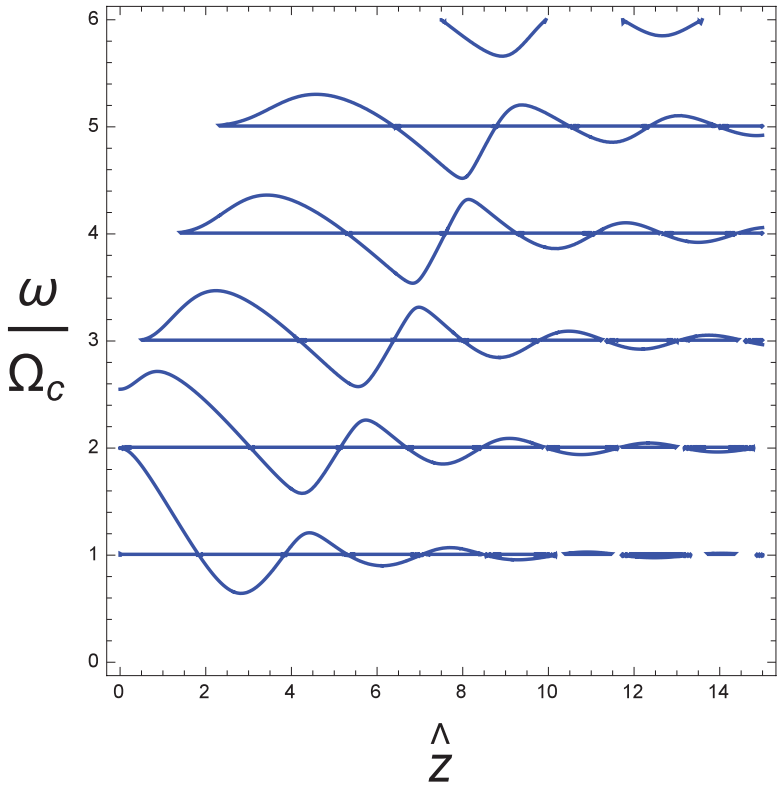

Fig. 1. The relation of ω_r/Ω_c and $\hat{z}$ for $\omega_{p_i}^2/\Omega_c^2 = 11.0$, where $\hat{z} = k_\perp \hat{v}_\perp/\Omega_c$ is a function of the wavelength and the magnetic field.

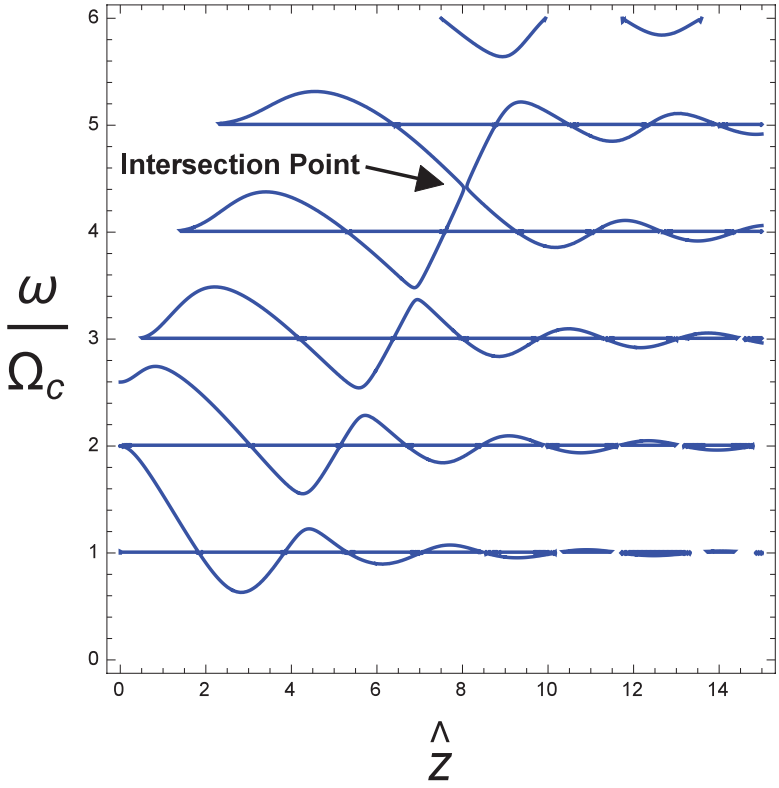

Fig. 2. The relation of ω_r/Ω_c and $\hat{z}$ for $\omega_{p_i}^2/\Omega_c^2 = 11.5$. The harmonics start to overlap where $\hat{z} = k_\perp \hat{v}_\perp/\Omega_c$.

plasma to gyro frequency ratios. Comparison of the electron Bernstein mode with the ion Bernstein mode shows that the ion mode tries to shift the threshold values for a weak magnetic field.

At $\omega_{pi}^2/\Omega_c^2 = 12$, the wave is unstable and the gaps generated between the harmonics become more prominent, as we can observe in Fig. 3. Now, we can reveal that there are gaps between harmonics by plotting the complex part of the frequency, as we have already considered that $\omega = \omega_r + i\omega_i$; this tells us about the imaginary part ω_i of the wave which disappears on the real frequency scale. The study of this complex part of the frequency gives an important result that the wave is growing in these specific regions, which means that, like the electron Bernstein mode, the ion Bernstein mode is also unstable for $\omega_{pi} > \Omega_c$; however, the numerical threshold value is greater than for the electron Bernstein wave. In the figures that follow, the solid lines show the real part and the dashed lines represent the imaginary part of the wave frequency ω.

The results obtained on increasing the value of the ratio ω_{pi}^2/Ω_c^2 from 12 to 15 are displayed in Fig. 4. These results can be directly compared with Bashir et al. [22] and Crawford [32]. The comparison reveals that the real frequency structure is similar, and unstable regions can be observed between the harmonics. The appearance of this inter-branch instability becomes more frequent as we increase the value of ω_{pi}^2/Ω_c^2. Figure 5 shows a group of inter-branch instabilities. There are unstable regions between the harmonics for the shorter-wavelength area. One of them is a non-resonating or purely growing mode for which $\omega_r = 0$ [32–34]. This mode occurs due to augmentation of the amplitude, but not with overlapping. In Fig. 5, it can be seen that the unstable regions are growing less, and the purely growing mode has a small domain. Figures 5 and 6 show harmonics for $\omega_{pi}^2/\Omega_c^2 = 50$ and $\omega_{pi}^2/\Omega_c^2 = 60$ respectively. With higher values of ω_{pi}^2/Ω_c^2, the domain of the purely growing mode also increases. One can also observe that the instabilities are affected by the value of the magnetic

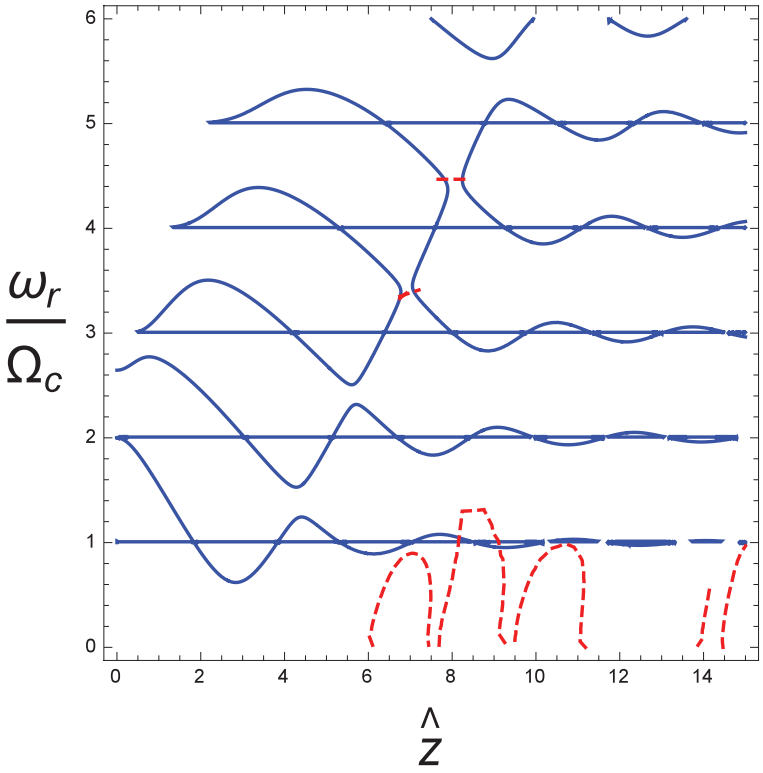

Fig. 3. The relation of ω_r/Ω_c and $\hat{z}$ for $\omega_{p_i}^2/\Omega_c^2 = 12.0$. The red dashed lines within the harmonics show the unstable regions.

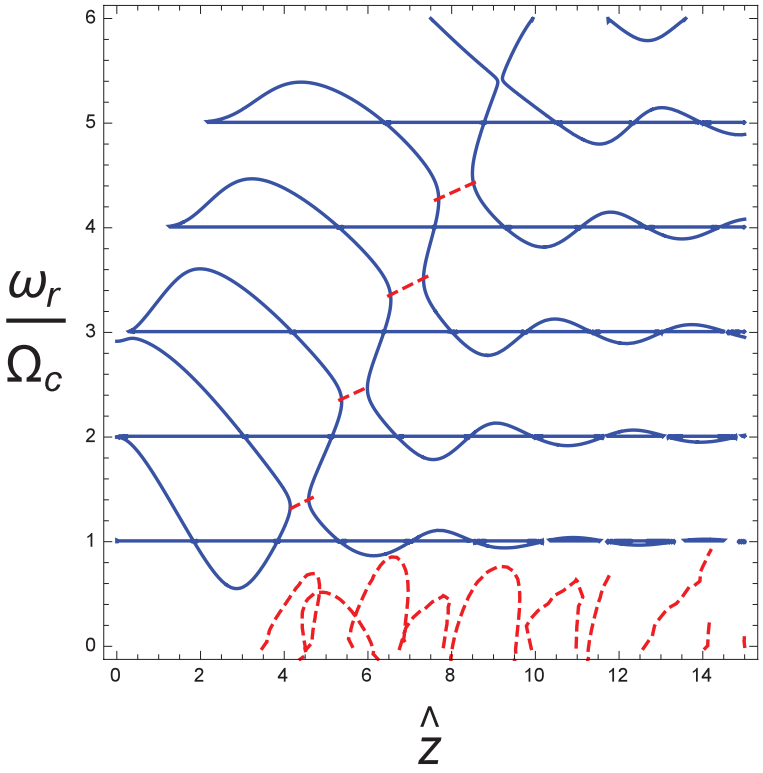

Fig. 4. The relation of ω_r/Ω_c and $\hat{z}$ for $\omega_{p_i}^2/\Omega_c^2 = 15.0$. The red dashed lines within the harmonics show the unstable regions.

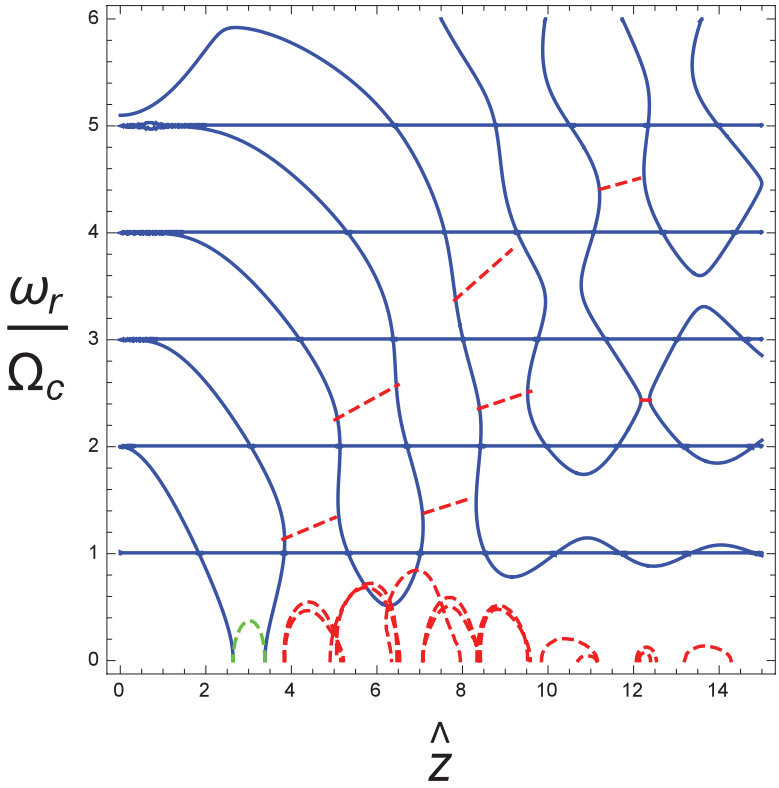

Fig. 5. The relation of ω_r/Ω_c and $\hat{z}$ for $\omega_{p_i}^2/\Omega_c^2 = 50$. The red dashed lines within the harmonics show the unstable regions, and their respective imaginary parts are also shown in red. The green color shows the purely growing part where $\omega_r = 0$.

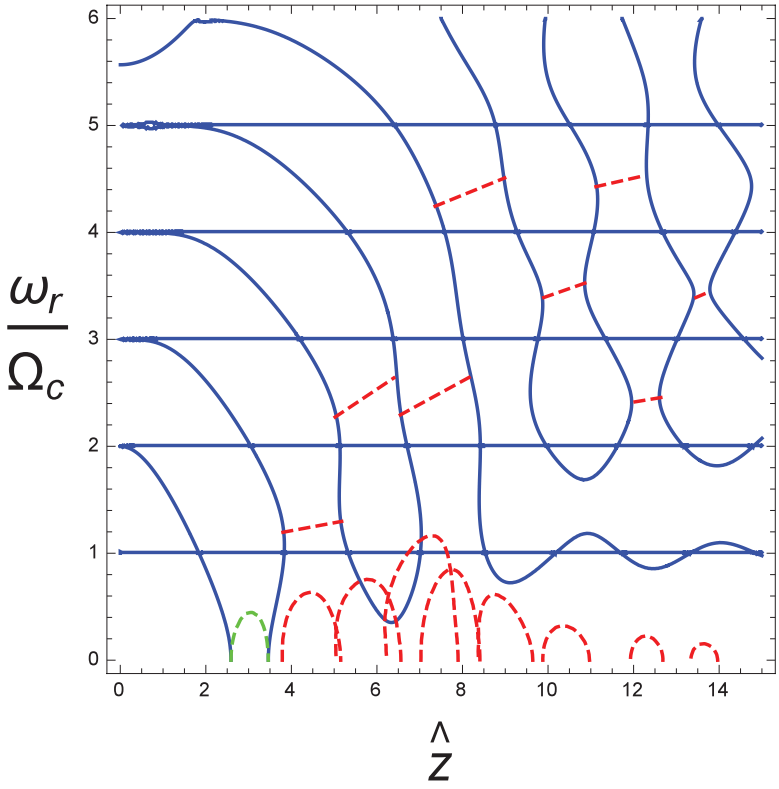

Fig. 6. The relation of ω_r/Ω_c and $\hat{z}$ for $\omega_{p_i}^2/\Omega_c^2 = 60$. The trend is the same as in Fig. . The purely growing mode where $\omega_r = 0$ is shown in the green color.

field. Decreasing the value of the magnetic field increases the anisotropy, which agrees with the high-frequency Bernstein mode instability case [22].

The above discussion draws a complete picture of the instabilities at different values of the argument. On comparison with the electron Bernstein wave, the ion Bernstein wave has a high threshold value with a low frequency. The direct correlation between value of $\omega_{pi}^2/\,\Omega_c^2$ and the overlapping of wave branches shows that the instability grows with a decreasing value of the magnetic field, and the wave becomes unstable at a high density. The distribution function provides free energy, which is the cause of wave instability. Nsengiyumva et al. [26] discussed the ion Bernstein mode with a kappa distribution function, and according to Ref. [26] the unstable regions shifted to a higher wavenumber or a lower wavelength by decreasing kappa (κ_i); this is in good agreement with the results for the ring velocity distribution function. This comparison shows that the ring velocity distribution reveals the instability of the Bernstein mode earlier than the kappa distribution function. The Bernstein mode is a current-driven mode and produces a heating effect [36–38]. Electrostatic waves are observed in pulsars, and there are a number of trapped modes present in pulsars. This discussion will be useful in any future treatment of radiation data from pulsars.

References

[1] R. A. Cairns, Proc. Spherical Tokamak Workshop on Bernstein Mode Heating and Current Drive (2003).
[2] A. K. Ram, Europhys. Conf. Abstr. **27A**, P-3.204 (2003).
[3] D. E. McGregor, R. A. Cairns, C. N. Lashmore-Davies, and M. O'Brien, Europhys. Conf. Abstr. **28G**, P-1.108 (2004).
[4] E. P. Gross, Phys. Rev. **82**, 232 (1951).
[5] H. K. Sen, Phys. Rev. **88**, 816 (1952).
[6] I. B. Bernstein, Phys. Rev. **109**, 10 (1958).
[7] F. W. Crawford and J. A. Tataronis, J. App. Phys, **36**, 2930 (1965).
[8] K. J. Harker, and F. W. Crawford, J. Appl. Phys. **39**, 5959 (1968).
[9] A. K. Ram, A. Bers, and C. N. Lashmore-Davies, Phys. Plasmas **9**, 409 (2002).
[10] D. A. Keston, E. W. Laing, and D. A. Diver, Phys. Rev. E **67**, 036403 (2003).
[11] E. W. Laing and D. A. Diver, Phys. Rev. E **72**, 036409 (2005).
[12] P. C. Efthimion, J. C. Hosea, R. Kaita, R. Majeski, and G. Taylor, Rev. Sci. Instrum. **70**, 1018 (1999).
[13] F. Deeba, Z. Ahmad, and G. Murtaza, Phys. Plasmas **17**, 102114 (2010).
[14] M. Ali, A. Hussain, and G. Murtaza, Phys. Plasmas **18**, 092104 (2011).
[15] F. Leuterer, Phys. Plasma **11**, 615 (1969).
[16] M. Moncuquet, N. Meyer-Vernet, S. Hoang, R. J. Forsyth, and P. Canu, J. Geophys. Res. **102**, 2373 (1997).
[17] R. L. Mace, Phys. Plasmas **10**, 2181 (2003).
[18] N. Meyer-Vernet, S. Hoang, and M. Moncuquet, J. Geophys. Res. **98**, 21163 (1993).
[19] D. D. Barbosa and W. S. Kruth, J. Geophys. Res. **85**, 08981 (1980).
[20] D. D. Barbosa, W. S. Kurth, D. A. Gurnett, and E. C. Sittler Jr., J. Geophys. Res. **98**, 19465 (1993).
[21] P. A. Bernhardt, C. A. Selcher, and S. Kowtha, J. Geophys. Res. Lett. **38**, L19107 (2011).
[22] M. F. Bashir, N. Noreen, G. Murtaza, and P. H. Yoon, Phys. Plasma Cont. Fusion **56**, 055009 (2014).
[23] C. S. Wu, D. Krauss-Varban, and T. S. Huo, J. GeoPhys. Res. **93**, 11527 (1988).
[24] S. P. Gary and C. D. Madland, J. GeoPhys. Res. **93**, 235 (1988).
[25] M. Vandas and P. Hellinger, Phys. Plasmas **22**, 062107 (2015).
[26] F. Nsengiyumva, R. L. Mace, and M. A. Hellberg, Phys. Plasmas, **20**, 102107 (2013).
[27] D. C. Montgomery and D. A. Tidman, *Plasma Kinetic Theory* (McGraw-Hill Press, New York, 1964).
[28] R. W. Fredricks, J. Geophys. Res. **76**, 5344 (1971).
[29] P. H. Yoon and R. C. Davidson, Phys. Rev. A **35**, 2619 (1987).
[30] F. F. Chen, *Introduction to Plasma Physics and controlled fusion* (Plenum Publishing Corporation, New York, 1984).

[31] N. A. Krall and A. W. Trivelpiece, *Principles of Plasma Physics* (McGraw-Hill Book Company, New York, 1973).
[32] M. Lazar, S. Poedts, R. Schlickeiser, and D. Ibscher, Sol. Phys. **289**, 369 (2014) [arXiv:1307.0768v1 [astro-ph.SR]] [Search INSPIRE].
[33] R. C. Davidson and C. S. Wu, Phys. Fluids **13**, 1407 (1970).
[34] F. Hadi, P. H. Yoon, and A. Qamar, Phys. Plasmas, **22**, 022112 (2015).
[35] F. W. Crawford, Radio Sci. J. Res. (NBS/USNC-URSI), **69D**, 789 (1965).
[36] Y. Y. Podoba, H. P. Laqua, G. B. Warr, M. Schubert, M. Otte, S. Marsen, and F. Wagner, Phys. Rev. Lett. **98**, 255003 (2007).
[37] A. Kuwahata, H. Igami, E. Kawamori, Y. Kogi, M. Inomoto, and Y. Ono, Phys. Plasmas, **21**, 102116 (2014).
[38] A. K. Ram and A. Bers, Phys. Plasmas, **9**, 409 (2002).